



## OPEN ACCESS

## EDITED BY

Li Wen,  
NSW Department of Planning, Industry  
and Environment, Australia

## REVIEWED BY

Lunche Wang,  
China University of Geosciences Wuhan,  
China  
Kaibo Wang,  
Chinese Academy of Sciences (CAS),  
China

## \*CORRESPONDENCE

Zhouping Shangguan,  
✉ shangguan@ms.iswc.ac.cn

RECEIVED 31 December 2022

ACCEPTED 19 May 2023

PUBLISHED 30 May 2023

## CITATION

Mao S and Shangguan Z (2023), Evolution  
of spatiotemporal patterns in vegetation  
net primary productivity and the driving  
forces on the Loess Plateau.  
*Front. Environ. Sci.* 11:1134917.  
doi: 10.3389/fenvs.2023.1134917

## COPYRIGHT

© 2023 Mao and Shangguan. This is an  
open-access article distributed under the  
terms of the [Creative Commons  
Attribution License \(CC BY\)](https://creativecommons.org/licenses/by/4.0/). The use,  
distribution or reproduction in other  
forums is permitted, provided the original  
author(s) and the copyright owner(s) are  
credited and that the original publication  
in this journal is cited, in accordance with  
accepted academic practice. No use,  
distribution or reproduction is permitted  
which does not comply with these terms.

# Evolution of spatiotemporal patterns in vegetation net primary productivity and the driving forces on the Loess Plateau

Shenglin Mao and Zhouping Shangguan\*

State Key Laboratory for Soil Erosion and Dryland Farming on the Loess Plateau, Northwest A&F University, Xianyang, Shaanxi, China

In this study, we determined whether changes in vegetation net primary productivity (NPP) can be used to characterize the quality of terrestrial ecosystems, which is critical for global change and carbon balance. We first explored the spatial correlation of NPP and its impact on vegetation restoration. MOD17A3 remote sensing products were used to analyze the temporal and spatial changes in NPP on the Loess Plateau (LP) over the last two decades (2000–2020). The resulting spatial autocorrelation indices identified cold and hot spots in the spatial clustering patterns. The effects of climate change and human activities on the anomalous clustering of NPP were assessed using Pearson correlation analysis and multi-temporal land use land cover data. The results indicate that i) Temporally, from 2000 to 2020, the NPP of the LP increased significantly by  $6.88 \text{ gCm}^{-2}\text{yr}^{-1}$  and so did the proportion of revegetated land area  $>400 \text{ gCm}^{-2}\text{yr}^{-1}$  from 4% to 37%. Spatially, NPP showed an increasing trend from northwest to southeast. ii) The vegetation NPP on the LP showed a strong positive global spatial autocorrelation ( $p < 0.01$ ). The hot and cold regions were polarized; the cold spots were clustered in the northwest, while the hot spots in the south and east. The spatial clustering patterns were dominated by high-high (HH) and low-low (LL) clusters. Abnormal patterns existed mainly in the transition areas between HH and LL clusters and insignificant regions, which were jointly affected by human activities and climate change. iii) Precipitation was the dominant climatic factor (86%) affecting the NPP variation in the LP, with the annual minimum precipitation showing a significantly positive relationship with the interannual variability in NPP, while the maximum precipitations greatly influenced the variation in local spatial anomaly patterns. This suggests that climatic extremes affect vegetation. Our study helps to facilitate green ecological management and high-quality development in the LP.

## KEYWORDS

net primary productivity, spatial autocorrelation, climate change, human activities, land use land cover, Loess Plateau

## 1 Introduction

Global warming has significantly affected the structure, processes, and functions of terrestrial ecosystems and regional ecological environment. As an important component of terrestrial ecosystems, vegetation provides essential materials for humans and plays an inestimable role in regulating climate change, supporting ecological environments, maintaining a carbon balance, and developing renewable resources. Vegetation net

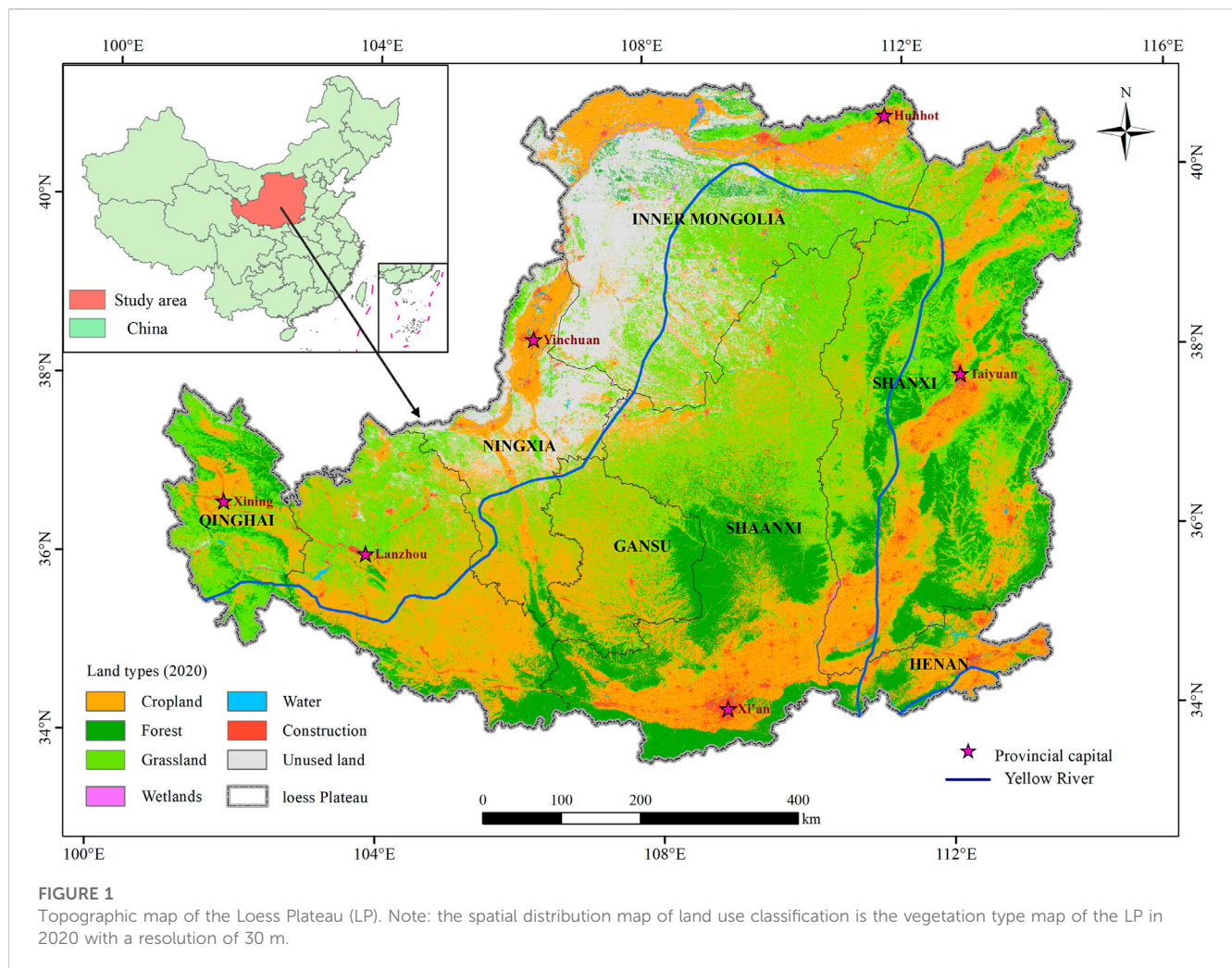
primary productivity (NPP) refers to the amount of organic carbon fixed by plant photosynthesis (GPP) minus the amount consumed by its respiration and growth (Goldewijk and Leemans, 1995; Yuan et al., 2021). NPP is an important index to measure the structure and function of terrestrial ecosystems and has been used in global and regional ecological environment monitoring and crop yield estimation (Wu et al., 2020; Zhang et al., 2022). Increasing carbon storage capacity may be the most effective way to limit global warming to 1.5°C. As a major factor in evaluating carbon sources and sinks, quantitative assessment of the dynamic changes in NPP not only expand our understanding of the interactions between climate change and ecosystems but also provides theoretical support for early realization of “carbon peaking” and “carbon neutrality” in ecologically fragile areas (Lei et al., 2020).

With the rapid development of remote sensing technology, the estimation of NPP may extend from sample plots to a regional or global scale. It is possible to evaluate the NPP of terrestrial ecosystems using field measurements and model validation; however, the cost of field surveys may be a major limitation. NPP has been a research hot spot at the regional level (Wu et al., 2014; Guo et al., 2021). Currently, the CASA model of the light energy utilization model (parametric model) and the MOD17A3HGF remote sensing product calculated using the BIOME-BGC model have been widely used (Wang et al., 2020; Li et al., 2021; Xiao et al., 2022). Guided by various international conventions on global climate change, the prohibition of deforestation has become a legal provision, and productivity estimates can only be obtained either directly from the field or via remote sensing data. Although the CASA model has recently been improved (Zhu et al., 2007; Pei et al., 2018), and the MOD17A3 HGF data have been refined from 500 m to 250 m, their reliability warrants improvement. In different natural environmental conditions in other regions, the application scope varies, while our understanding of the mechanism regulating various interactions of NPP remains rudimentary, thereby hindering parameter regulations (Kolby Smith et al., 2016). Therefore, there are errors in NPP estimations. A common method used in ecology and geology is the linear regression from the regional to pixel-by-pixel scale to reveal the temporal and spatial changes in vegetation NPP and its response to climate change. Cui et al. (2018) analyzed the growth trend in vegetation NPP in China from 1982 to 2011 based on the GLOPEM-CEVSA model, revealing a growth rate of  $5.66 \text{ gCm}^{-2} (10 \text{ yr})^{-1}$ . Previous studies have combined simple and multiple linear regression models to explore the spatial-temporal evolution and driving factors of NPP in national park vegetation restorations (Yang et al., 2023) and urbanization development (Peng et al., 2016). Additionally, methods such as partial correlation analysis and the Mann-Kendall trend test better reveal the spatiotemporal variation and driving forces in regional NPP (Pan and Dong, 2018; Wei et al., 2022). Classic statistical analysis suggests that spatiotemporal variation and driving forces of NPP are generally defined as “first-order effects” (Huang et al., 2013). However, spatial pattern changes can also be the result of local effects. Presently, the potential changes and effects of spatial heterogeneity and spatial autocorrelation of vegetation NPP in the Loess Plateau (LP) remains unclear. Therefore, to clarify the

spatial pattern in vegetation NPP, we used the first law of geography with spatial autocorrelation to characterize the spatial dependence and spatial heterogeneity of vegetation NPP and explore the convergence and divergence between spatially adjacent location data, i.e., “second-order effect” (Huang et al., 2013; Fan and Myint, 2014). This can better show the spatial variation laws of NPP in different regions.

LP is an important ecological barrier in China, which has one of the most serious soil erosion areas. Prior to the 1990s, China controlled soil erosion by constructing terraces and silt dams and implementing management projects for slopes and small watersheds. Since 2000, China has initiated large-scale projects such as the Grain for Green Project (GGP), gully control, and land reclamation. Thus, the rate of vegetation coverage increased from 31.6% in 1999 to 65% in 2017. In 2016, China has launched the first batch of pilot projects for the ecological protection of mountains, rivers, forests, fields, and lakes. State policies have continuously promoted the construction of rural revitalization and ecological civilization projects. Improving the vegetation coverage of the LP through natural restoration has achieved remarkable results. Although the Grain for Green Project has been implemented to alleviate the problems caused by human activities and natural factors, the local ecological environment remains very fragile, and problems such as insufficient vegetation carrying capacity are becoming increasingly prominent (He et al., 2006; Fu et al., 2011). Vegetation restoration has had several effects on this ecosystem (Lü et al., 2012; Zhao et al., 2013; Zhang et al., 2018), and the vegetation NPP of the LP has evident spatial heterogeneity with interannual variation. Prior to 1990, many scholars explored the changes in vegetation on LP in historical periods using pollen data and other technologies (Liu et al., 1996; Jiang and Ding, 2005). Given the severe soil and water loss, the correlation between vegetation restoration and soil environment after afforestation has been investigated using sample plots (Shangguan and Zheng, 2006). After 2000, remote sensing methods were used to reveal the changes in vegetation cover in the LP, and their association with climate and social factors and also analyze the influencing factors of vegetation change (Chen et al., 2007). At the plot scale, the interaction and mechanism between vegetation and soil erosion, soil and water conservation and organic carbon has attracted attention. The relationship between water and vegetation has been well demonstrated. How to limit the dry layer of soil and sustainably manage regional vegetation has become a hot research topic (Zhang et al., 2016; Ma et al., 2022).

Data on the spatial autocorrelation of vegetation NPP on the LP are limited. We hypothesize that the vegetation NPP on LP has a spatial autocorrelation and correlates with natural factors and human activities. Therefore, we aimed to (1) reveal the temporal and spatial distribution patterns and NPP variation on the LP from 2000 to 2020, (2) explore the spatial dependence and heterogeneity of NPP in the LP from 2000 to 2020 by exploiting global and local autocorrelations, and (3) quantify the impact and contribution of climatic factors and human activities on NPP using Pearson correlation analysis and the land use transition matrix. Our results provide important information to better manage ecological resources for successful vegetation restoration in various regions of the LP and can help to facilitate high-quality development in the LP.



## 2 Materials and methods

### 2.1 Study area

The LP is located in the middle of the Yellow River basin ( $33^{\circ}41' - 41^{\circ}16'N$ ,  $100^{\circ}52' - 114^{\circ}31'E$ ), with a total area of approximately  $6.4 \times 10^5 \text{ km}^2$ , spanning the provinces of Gansu, Henan, Inner Mongolia, Ningxia, Qinghai, Shanxi, and Shaanxi in China (Figure 1). The overall topography of the LP presents a downward trend of high in the northwest and low in the southeast. It is located in the semi-humid and semi-arid regions of China, with typical temperate continental monsoon climate characteristics. The multi-year average temperature and precipitation are approximately  $8^{\circ}\text{C}$  and 400 mm, respectively. The heavy and concentrated rainstorms in summer, coupled with high evaporation, high sediment content in the water system, and loose loess soil, cause serious soil erosion. According to the national classification standard of China, we used the land use data set of 2000–2020 produced by Zhang et al. (2021), and divide the land use types of LP into grassland, cultivated, forest, and unused lands, construction land, and wetland and water areas. In recent decades, the implementation of restoration projects (such as the Grain for Green project), rapid urbanization, and global

warming have significantly altered the vegetation cover and land structure of the LP (Song et al., 2014), impacting the regional ecological environment.

### 2.2 Data description and preprocessing

#### 2.2.1 NPP

The NPP data are based on the MODIS satellite-generated MOD17A3HGF V006 product provided by NASA (<https://lpdaac.usgs.gov/products>), which provides annual NPP information at the 500-m pixel resolution. Annual NPP was derived from the addition of all 8-day net photosynthesis (PSN) products (MOD17A2H) for a given year, calculated using the BIOME-BGC model to derive the global terrestrial vegetation NPP interannual data. Previous research has verified the reliability of the MOD17A3 NPP data with the measured data used in the analysis of the study area (Liu et al., 2018; Li et al., 2020). We used the MODIS Reprojection Tool (MRT) and ArcGIS 10.8 software to eliminate outliers and invalid values, and uniformly cropped data from the LP area. Due to the elimination of cloud pollution, we used the nearest neighbor method to resample a 1 km dataset in our analysis.

**TABLE 1** Classification of the land use land cover (LULC) dataset used in this study.

Primary classes	Sub-classes
Cropland	Rainfed cropland
	Herbaceous cover
	Irrigated cropland
Forest	Open evergreen broadleaved forest
	Closed evergreen broadleaved forest
	Open deciduous broadleaved forest (0.15 < fc < 0.4)
	Closed deciduous broadleaved forest (fc > 0.4)
	Open evergreen needle-leaved forest (0.15 < fc < 0.4)
	Closed evergreen needle-leaved forest (fc > 0.4)
	Closed deciduous needle-leaved forest (fc > 0.4)
	Shrubland
	Deciduous shrubland
	Unused land
Unconsolidated bare areas	
Permanent ice and snow	
Sparse vegetation (fc < 0.15)	
Grassland	Grassland
Wetlands	Wetlands
Impervious surfaces	Impervious surfaces
Water	Waterbody

### 2.2.2 Meteorological data

The meteorological data (1 km × 1 km) were originated from the LP Sub Center, National Earth System Science Data Center of China (<http://loess.geodata.cn>), which generates monthly temperature and precipitation data for China from 2000 to 2020 using a Delta spatial downscaling scheme. The LP region was generated via mask extraction.

### 2.2.3 Land use land cover (LULC)

The multi-temporal land use land cover dataset was obtained from the Institute of Aerospace Information Research, Chinese Academy of Sciences (<https://doi.org/10.5194>), which produces global 30-m land-cover results every 5 years, from 1985 to 2020 on the Google Earth Engine platform using all Landsat satellite data from 1984 to 2020. The overall accuracy of this dataset is >80% (Zhang et al., 2021); hence, we used it in this study. We selected land-cover data from 2000 to 2020 (i.e., 2000, 2005, 2010, 2015, and 2020) for the dynamic study of NPP on LP by tailoring the data. A field investigation combined with the actual land types of the LP enabled us to divide the dataset into the seven categories, with an overall validation accuracy of 96.4% (Table 1). According to the classification standard of Zhang et al.'s data set and the actual land types of the LP, we reclassified the land types into seven types.

## 2.3 Methods

The fishing net (10 km × 10 km) was created using the processed NPP data, following which the NPP of each matrix unit was assigned using the partitioned table. Finally, the global spatial autocorrelation test was performed in ArcGIS on the NPP data of the LP from 2000 to 2020. If the results showed a significant global correlation, then a local spatial autocorrelation analysis was performed.

### 2.3.1 Global spatial autocorrelation

The global Moran's I index and high/low clustering (Getis-Ord General G) characterized whether the NPP of the LP from 2000 to 2020 had clustered or outliers in space (Swetnam et al., 2015; Cheniti et al., 2021). The formula for calculating the global Moran's I index is as follows:

$$I = \frac{\left\{ \sum_{i=1}^n \sum_{j \neq i}^n w_{ij} (x_i - \bar{x})(x_j - \bar{x}) \right\}}{S^2 \sum_{i=1}^n \sum_{j \neq i}^n w_{ij}}, \quad (1)$$

$$S^2 = \sum_i (x_i - \bar{x})^2 / n, \quad (2)$$

where  $n$  is the total number of observation elements,  $x_i$  and  $x_j$  are the pixel values of NPP at positions  $i$  and  $j$  ( $i \neq j$ ),  $\bar{x} = \left( \sum_i x_i \right) / n$ ,  $i$  is a variance, and  $w_{ij}$  is a symmetric spatial weight matrix element; if  $i$  is adjacent to  $j$ , then  $w_{ij}$  is 1, otherwise  $w_{ij}$  is 0.

To test the significance of the spatial autocorrelation relationship, the standardized statistic  $Z$  value was introduced. The calculation formula of  $Z$  is:

$$Z = \frac{(I - E(I))}{\sqrt{\text{VAR}(I)}}, E(I) = -\frac{1}{(n-1)}, \quad (3)$$

where  $E(I)$  is the expected value of  $I$  (compared with Moran's I index),  $\text{VAR}(I)$  is the variance of the variable  $I$ ,  $\text{VAR}(I) = E(I^2) - E(I)^2$ . Moran's I index is generally between  $-1$  and  $1$ . A Moran's I index and  $Z$  value greater than  $0$  and significant (with a  $p$ -value within the given significance level) indicates a positive spatial correlation. Therefore, similar observations (high or low) tend to be spatially clustered. When the values are equal to  $0$ , the values are independent and randomly distributed.

The General G and its expected value  $E(G)$  and  $Z$ -score are calculated as follows:

$$G = \frac{\left( \sum_{i=1}^n \sum_{j=1}^n w_{ij} x_i x_j \right)}{\sum_{i=1}^n \sum_{j \neq i}^n x_i x_j},$$

$$Z = \frac{\{G - E(G)\}}{\sqrt{\text{VAR}(G)}}. \quad (4)$$

If General G is greater than  $E(G)$ , and the  $Z$ -score is positive, then the high NPP values will cluster within the region. If General G is less than  $E(G)$ , and the  $Z$ -score is negative, then the low NPP values will tend to cluster.

### 2.3.2 Local spatial autocorrelation

To explore whether the high and/or low local spatial observations were concentrated, we used the Hot Spot Analysis (Getis-Ord  $G_i^*$ ) and Anselin Local Moran's I tools in ArcGIS 10.8 to perform a local spatial autocorrelation analysis. Getis-Ord  $G_i^*$  identified statistically significant hot and cold

spots (Getis and Ord, 2010). Anselin Local Moran’s I identified spatial clusters of features with high or low values, as well as spatial outliers (Anselin, 1995; Liu K. et al., 2022).

The Getis-Ord  $G_i^*$  is as follows:

$$G_i^* = \frac{(\sum_{j=1}^n w_{ij}x_j - \bar{X}\sum_{j=1}^n w_{ij})}{S\sqrt{[n\sum_{j=1}^n w_{ij}^2 - (\sum_{j=1}^n w_{ij}x_j)^2] / (n-1)}} \tag{5}$$

$$\bar{X} = \frac{(\sum_{j=1}^n x_j)}{n} \tag{6}$$

$$S = \sqrt{\frac{(n\sum_{j=1}^n x_j^2)}{n} - (\bar{X})^2} \tag{7}$$

where  $x_i$  is the same as the Formula (1), and the  $G_i^*$  statistic uses the z-score. For statistically significant values, positive and highest z-score indicates that the areas with high NPP are more closely clustered (hot spots). Conversely, a negative and low z-score means that the areas with low NPP are more tightly clustered (cold spots). The Anselin Local Moran’s I statistic is defined as:

$$I_i = \frac{[(x_i - \bar{x})\sum_{j=1, j \neq i}^n w_{ij}(x_j - \bar{x})]}{S_i^2} \tag{8}$$

$$S_i^2 = \frac{(\sum_{j=1, j \neq i}^n w_{ij})}{(n-1)} - \bar{X}^2 \tag{9}$$

The standardized statistic for the Anselin Local Moran’s I statistical test is similar to the global Moran’s I index and distinguishes statistically significant clusters of high values (HH), clusters of low values (LL), outliers (HL) where high values are mostly surrounded by low values, and outliers (LH) where low values are mostly surrounded by high values.

### 2.3.3 Pearson correlation analysis

Pearson correlation analysis is used to determine the linear correlation between multiple variables and ranges from -1 to 1 (Gbagir et al., 2022). The MATLAB R2021 software generated the codes to analyze the pixel-by-pixel correlations between NPP

temperature and NPP rainfall, as well as the regional contribution of temperature and rainfall to NPP. The correlations were combined with spatial autocorrelations to analyze the spatial anomalous changes in vegetation NPP. The correlation coefficient  $r_{xy}$  is calculated as follows:

$$r_{xy} = \frac{\{\sum_{i=1}^n [(x_i - \bar{X})(y_i - \bar{Y})]\}}{\sqrt{\sum_{i=1}^n (x_i - \bar{X})^2 \sum_{i=1}^n (y_i - \bar{Y})^2}} \tag{10}$$

where,  $n$  is the number of years in the monitoring period ( $n = 21, i = 1, 2, \dots, 21$ ),  $x_i$  is NPP of the 1 km raster data in different years,  $\bar{X}$  is the average of 21 years of NPP raster data,  $y_i$  is the raster data of temperature or precipitation in different years, and  $y_i$  is the raster data of the annual average rainfall or temperature.

## 3 Results

### 3.1 Temporal and spatial distribution pattern of NPP in the Loess Plateau

The annual mean value of vegetation NPP on the LP from 2000 to 2020 followed a fluctuating upward trend ( $p < 0.05$ ), with a growth rate of  $6.88 \text{ gCm}^{-2}\text{yr}^{-1}$ . The increases prior to 2010 (3.61%) were more pronounced than those after (1.75%). The multi-year average NPP was  $298.59 \text{ gCm}^{-2}\text{yr}^{-1}$ . The total volume of NPP increased from 127.12 Tg (in 2000) to 212 Tg (in 2020), with an annual growth rate of  $4.05 \text{ Tg/yr}$ . The mean NPP varied in different years, with 2002 being the lowest at only  $201.64 \text{ gCm}^{-2}\text{yr}^{-1}$ , while the highest was in 2018. Before 2012, the average annual NPP of the LP was lower than the multi-year average; however, in 2012, it increased sharply to  $338.13 \text{ gCm}^{-2}\text{yr}^{-1}$  (Figure 2).

Three obvious mutation periods were more intense than other years, namely 2001 to 2002, 2011 to 2012, and 2017 to 2018. The average annual NPP of each province in the LP from 2000 to 2020 is listed in Table 2. Henan Province had the highest average annual NPP ( $391.57 \text{ gCm}^{-2}\text{yr}^{-1}$ ) and the largest growth rate ( $+11.60 \text{ gCm}^{-2}\text{yr}^{-1}$ ), followed by Shaanxi, Shanxi, Gansu, Ningxia, Inner Mongolia, and Qinghai (with a growth rate of  $5.10 \text{ gCm}^{-2}\text{yr}^{-1}$ ). The NPP of each province showed rapid growth from 2000 to 2020, and the time points of NPP mutation in the LP, aligned with the implementation of the Grain for Green project in 1999. All provinces actively responded to the Grain for Green project with rapid vegetation restoration on the LP, achieving remarkable results.

The inter-annual NPP of the LP presented a spatial distribution pattern of low in the northwest and high in the southeast. The areas with the highest NPP were situated primarily in the central and southeast LP (Figure 3). Approximately 16%–55% of the total area had an average annual NPP below  $200 \text{ gCm}^{-2}\text{yr}^{-1}$ , which decreased annually, but the regional annual average NPP did not vary and remained at  $200\text{--}400 \text{ gCm}^{-2}\text{yr}^{-1}$ . The proportion of NPP with an average of  $400\text{--}600 \text{ gCm}^{-2}\text{yr}^{-1}$  varied significantly between years, encompassing only 4% in 2000 compared with the 37% in 2020, demonstrating significant improvements over time (Figure 4).

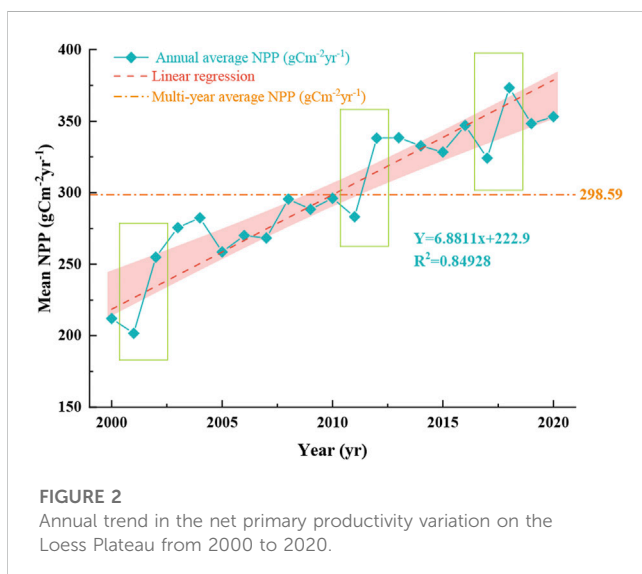


FIGURE 2 Annual trend in the net primary productivity variation on the Loess Plateau from 2000 to 2020.

TABLE 2 Annual average net primary productivity of each province in the Loess Plateau from 2000 to 2020 ( $gCm^{-2}yr^{-1}$ ).

Year	Henan	Shaanxi	Shanxi	Gansu	Qinghai	Ningxia	Inner Mongolia
2000	320.42	228.24	276.56	215.11	252.84	122.88	111.82
2001	281.25	221.75	229.47	238.26	270.01	134.42	101.29
2002	317.77	293.96	277.45	301.17	303.83	179.85	143.15
2003	402.07	316.04	333.88	288.42	293.88	181.09	153.17
2004	419.64	323.01	349.29	290.74	285.99	179.73	158.93
2005	365.51	300.65	303.10	296.23	302.84	156.06	128.13
2006	400.08	317.67	327.60	290.50	304.47	158.59	135.79
2007	374.77	315.27	301.30	303.58	324.43	172.11	144.22
2008	397.02	344.23	357.23	328.79	323.41	170.00	154.30
2009	387.30	345.69	342.54	311.01	321.94	172.80	152.16
2010	384.23	366.80	334.74	329.26	332.21	201.29	147.30
2011	359.81	346.13	341.58	303.46	309.21	181.71	136.08
2012	436.90	404.03	396.57	365.32	315.07	229.35	196.28
2013	370.08	407.89	392.81	385.80	341.97	224.63	183.65
2014	370.86	401.49	386.14	377.79	316.25	236.59	179.20
2015	452.12	410.42	377.65	372.73	302.86	209.22	165.26
2016	424.77	407.33	426.40	357.69	341.23	221.98	204.56
2017	411.21	393.01	376.62	356.51	321.38	215.23	177.82
2018	487.61	448.47	429.72	423.61	355.85	255.01	201.51
2019	384.19	410.11	381.09	412.45	358.75	251.88	205.03
2020	475.10	420.87	420.78	399.85	339.85	226.78	178.95
Mean	391.57	353.50	350.62	330.88	315.16	194.34	159.93

Our results also indicated that before 2002, there were almost no areas with an average NPP above  $600 gCm^{-2}yr^{-1}$ , which has gradually increased over the past 20 years. Therefore, the implementation of ecological construction projects (such as the project of grain for green project) has improved the vegetation on the LP and the ecological environment has achieved remarkable results.

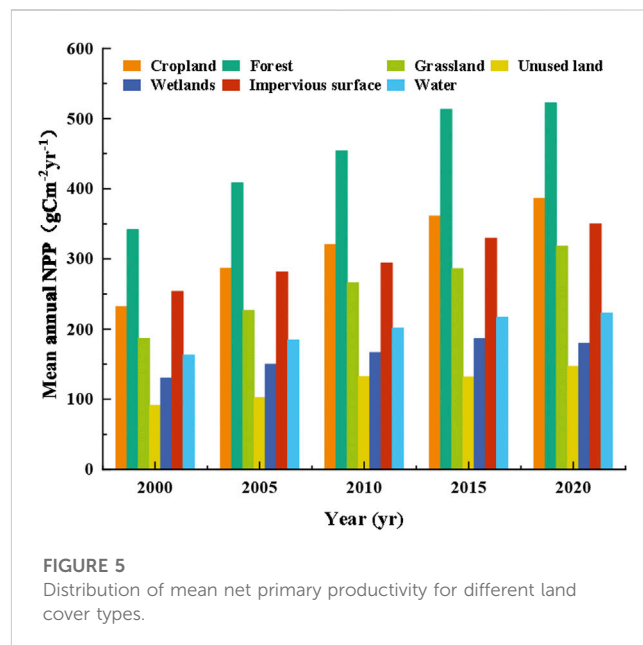
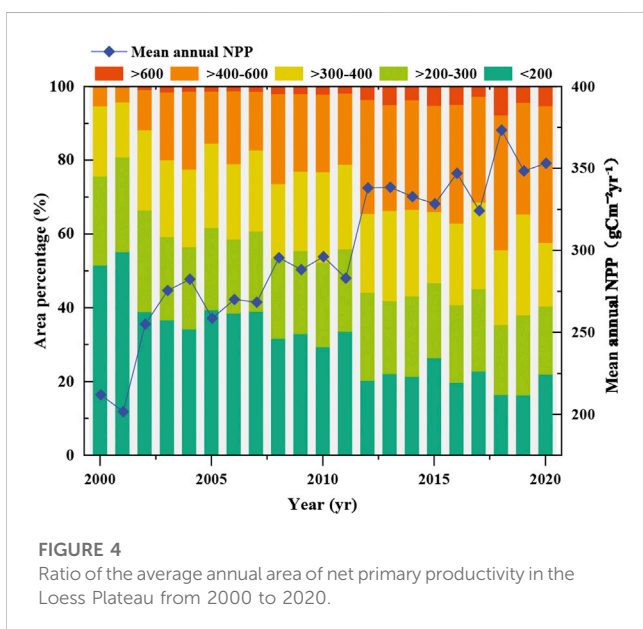
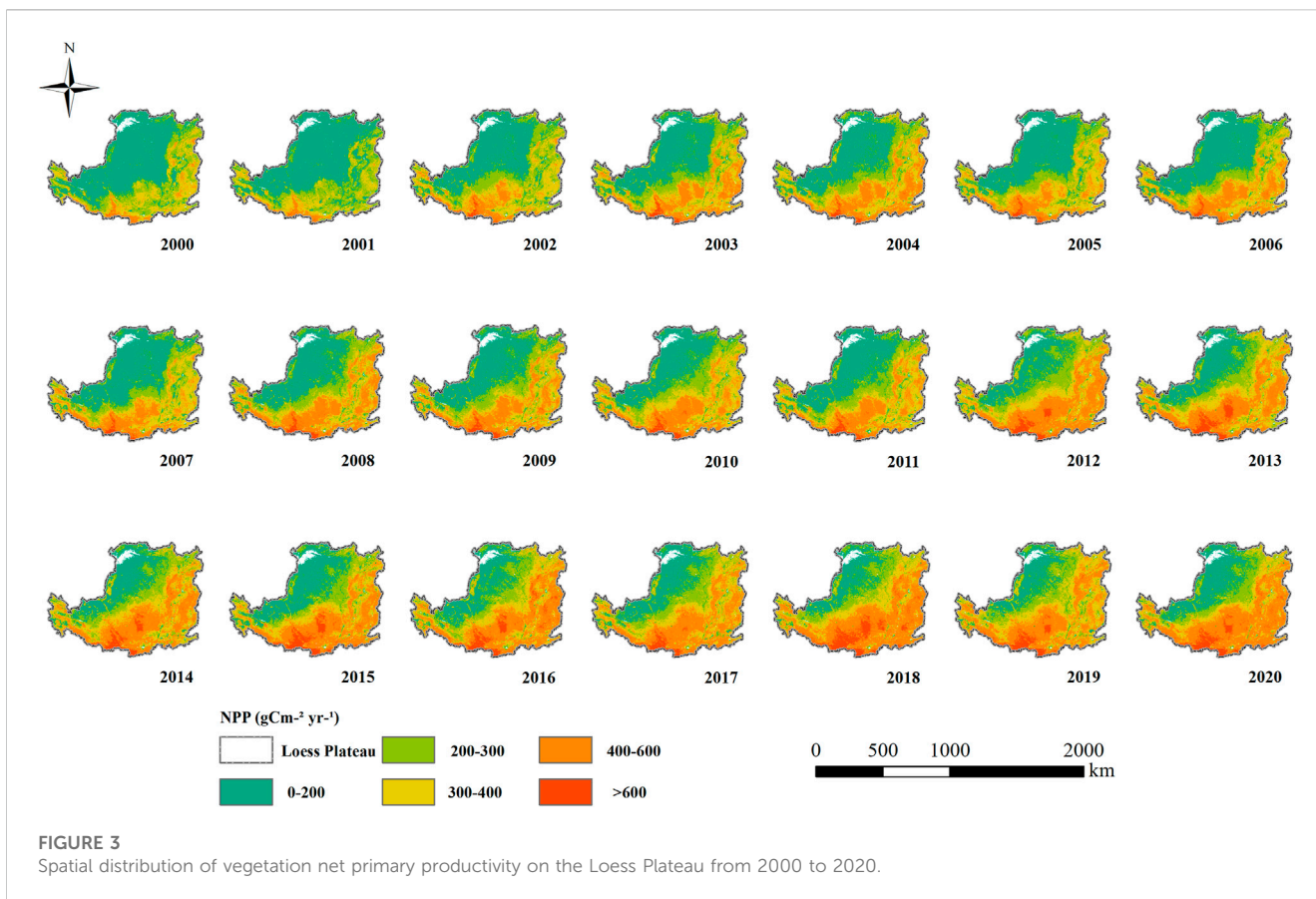
The land cover variations impacted the terrestrial ecosystem structure. The variations in NPP of different vegetation types from 2000 to 2020 are illustrated in Figure 5. The mean NPP values of different vegetation types (from high to low) were: forest ( $447.87 gCm^{-2}yr^{-1}$ ) > cropland ( $317.20 gCm^{-2}yr^{-1}$ ) > impervious surface ( $301.61 gCm^{-2}yr^{-1}$ ) > grassland ( $256.81 gCm^{-2}yr^{-1}$ ) > water ( $197.79 gCm^{-2}yr^{-1}$ ) > wetlands ( $162.56 gCm^{-2}yr^{-1}$ ) > unused land ( $194 gCm^{-2}yr^{-1}$ ). All types showed a significant increasing trend from 2000 to 2020. Among them, the annual average NPP of the forest was much higher than that of other land types, indicating that the forest ecosystem is a large carbon sink (Figure 5). Moreover, there were significant discrepancies in the total annual NPP among different vegetation types. The annual total NPP of cropland, forest, and grassland increased rapidly above 40 TgC, while the total NPP of unused

land was much higher than that of the remaining land, which suggests the carbon sequestration potential of unused land is enormous.

## 3.2 Spatial autocorrelation analysis

### 3.2.1 Global autocorrelation variations of NPP

Global spatial autocorrelations explore the spatial agglomeration characteristics of carbon sequestration of vegetation NPP on the LP. As listed in Table 3, we calculated the global Moran's I index, General G, and their z-scores, expectation values, variance, and p-value of NPP from 2000 to 2020. The annual global Moran's I index varied from 0.95 to 0.97, and the Moran's I index of the multi-year average NPP was 0.961, extremely close to 1. At the same time, the Z-score of each year was positive and above 106 ( $Z(I) > 2.58$ ), indicating that the NPP of the LP in 2000–2020 showed a very significant agglomeration effect on the interannual spatial distribution and had a strong positive spatial correlation ( $p < 0.01$ ). Correspondingly, the annual General G was greater than  $E(G)$  ( $p$ -value  $< 0.001$ ), and  $Z(d)$  was also much higher than 2.58 [ $P(G) < 0.01$ ], which



indicated that the overall spatial distribution pattern of NPP in the study area had high clustering. The global autocorrelation did not reveal the specific clustering pattern at the fine scale; therefore, the local Moran's I was needed to further identify the spatial clustering pattern of NPP.

### 3.2.2 Hot spot analysis and local autocorrelation of NPP

The hot spot analysis tool identified the statistically significant hot and cold areas of NPP in the LP. The hot and

TABLE 3 Global autocorrelation of net primary productivity in the Loess Plateau from 2000 to 2020.

Year	Moran's I	Z (I)	p-value	General G	E(G)	Z(d)	P(G)
2000	0.953	106.837	<0.01	0.000192	0.000153	102.359	<0.01
2001	0.947	106.215	<0.01	0.000191	0.000153	101.847	<0.01
2002	0.950	106.530	<0.01	0.000183	0.000153	100.919	<0.01
2003	0.952	106.826	<0.01	0.000186	0.000153	101.643	<0.01
2004	0.957	107.323	<0.01	0.000185	0.000153	102.026	<0.01
2005	0.962	107.857	<0.01	0.000191	0.000153	103.292	<0.01
2006	0.962	107.942	<0.01	0.000191	0.000153	103.363	<0.01
2007	0.958	107.494	<0.01	0.000186	0.000153	102.333	<0.01
2008	0.962	107.934	<0.01	0.000187	0.000153	102.755	<0.01
2009	0.958	107.414	<0.01	0.000186	0.000153	102.258	<0.01
2010	0.962	107.900	<0.01	0.000185	0.000153	102.483	<0.01
2011	0.960	107.715	<0.01	0.000187	0.000153	102.662	<0.01
2012	0.962	107.922	<0.01	0.000179	0.000153	101.458	<0.01
2013	0.964	108.144	<0.01	0.000183	0.000153	102.397	<0.01
2014	0.956	107.178	<0.01	0.000180	0.000153	100.874	<0.01
2015	0.965	108.285	<0.01	0.000188	0.000153	103.265	<0.01
2016	0.956	107.211	<0.01	0.000178	0.000153	100.616	<0.01
2017	0.959	107.519	<0.01	0.000179	0.000153	101.104	<0.01
2018	0.969	108.638	<0.01	0.000179	0.000153	101.932	<0.01
2019	0.954	107.056	<0.01	0.000176	0.000153	99.730	<0.01
2020	0.970	108.742	<0.01	0.000182	0.000153	102.760	<0.01
Mean	0.961	107.373	<0.01	0.000184	0.000153	101.424	<0.01

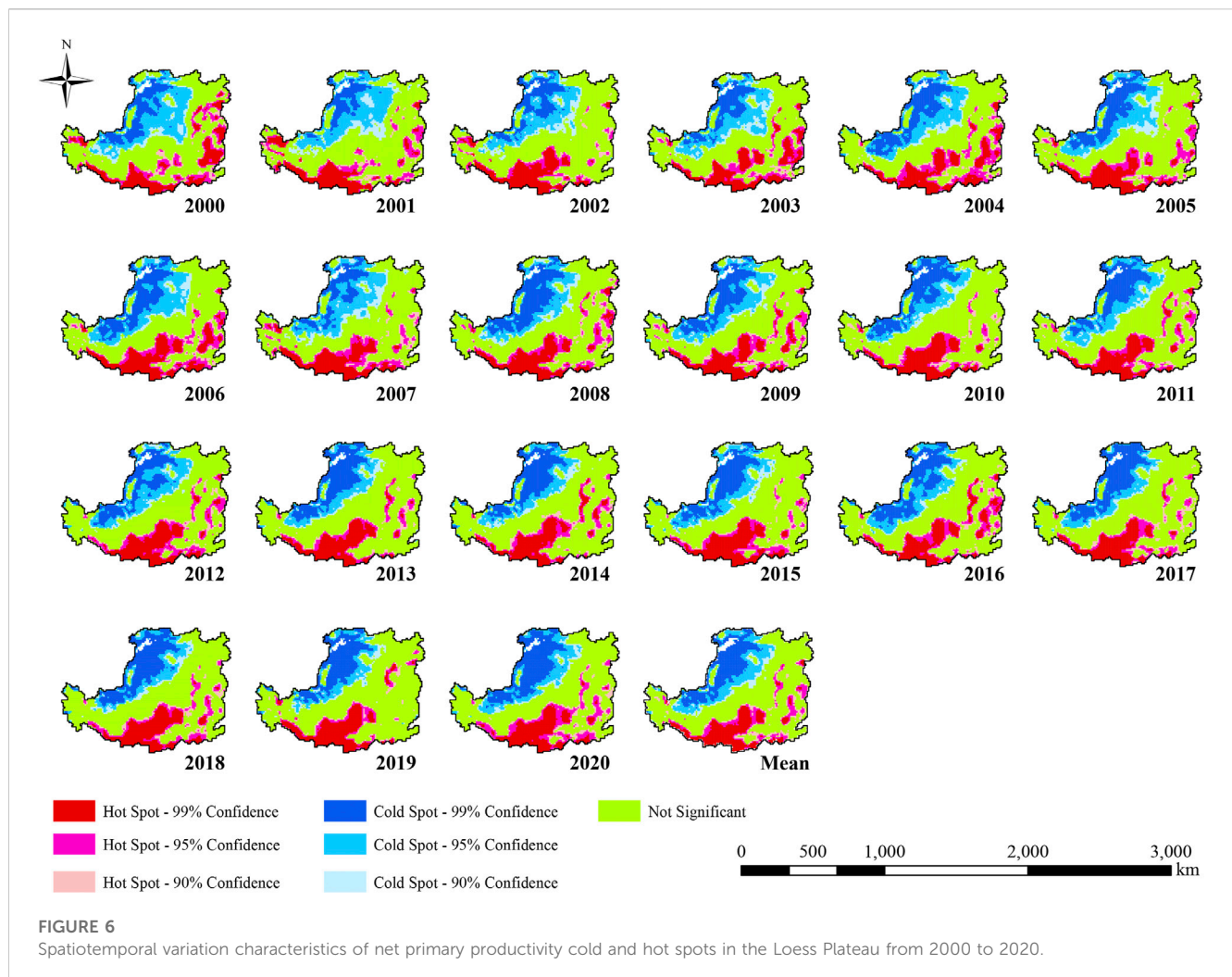
cold spot areas were polarized. The cold spots were mainly distributed in the northwest of Ningxia, Inner Mongolia (Ordos and Bayannur), and Gansu (Lanzhou and Baiyin), while the hot spots were distributed in the southern and eastern regions, mainly covering Gansu (Tianshui, Pingliang, Qingyang), central Shaanxi, and Henan (Sanmenxia, Luoyang).

From 2000 to 2020, the overall distribution pattern of the cold spot areas did not vary, but the area containing an NPP with a 99% confidence level gradually expanded and incorporated Ordos City, Inner Mongolia. In addition, the cold spot area of the Yulin City started to gradually disappear in 2009, while the cities of Bayannur and Shizuishan changed from insignificant to cold spot areas. There were also local anomalies in Lanzhou's NPP in 2007, 2018, and 2019 (Figure 6).

The cold spot area (at the 99% confidence level) showed an increasing trend and its proportion increased to 15%. The cold spot area gradually decreased at 95% and 90% confidence levels. However, the insignificant areas remained dominant, accounting for 41%–50%. Conversely, the hot spot areas were stable at the 99%, 95%, and 90% confidence levels, accounting for approximately 11%, 8.5%, and 5.4%, respectively, indicating

that the hot spot areas were transferred into different spatial locations. For instance, the NPP in the south of the hot spot area gradually expanded from 2000 to 2020, from Tianshui, Baoji, and Xi'an to Xianyang, Pingliang, and Yan'an. Other hot spots were sporadically distributed in Shanxi and Henan Province, and the high NPP pattern in the eastern region (Changzhi, Jincheng, Jinzhong City) almost disappeared in 2002, 2007, 2010, and 2019. Generally, the hot spots of NPP in the eastern region are likely to continue to shrink.

To further identify the specific clustering patterns of hot and cold areas, clustering and outlier analyses were performed. The NPP had spatial heterogeneity in the spatial distribution and the inter-annual local spatial pattern was dominated by the HH and LL clustering patterns; the clustering model of the multi-year average vegetation NPP was similar to each year (Figure 7). HH was mainly distributed in southeastern Gansu, southern Shaanxi, and central Henan (which encompasses 16%–22% of the area of the LP). The LL was concentrated in the Inner Mongolia Autonomous Region, northern Ningxia, northwestern Gansu, and northeastern Shaanxi (23%–30%). The gray areas were insignificant, accounting for 50%–60%, revealing no spatial autocorrelation patterns (Figure 7).



### 3.3 Climatic factors affecting vegetation NPP changes

To further explore the spatial-temporal variations and spatial anomalous clustering changes in vegetation NPP, we analyzed the responses of precipitation and temperature to vegetation NPP.

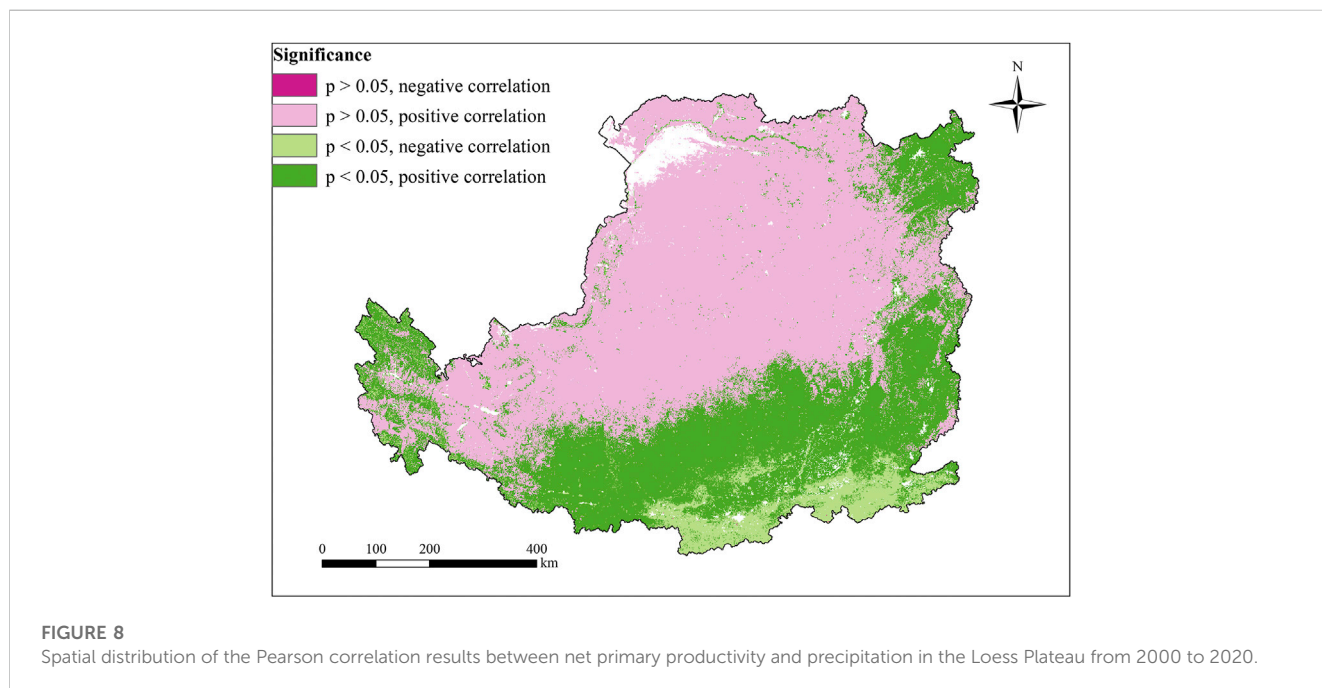
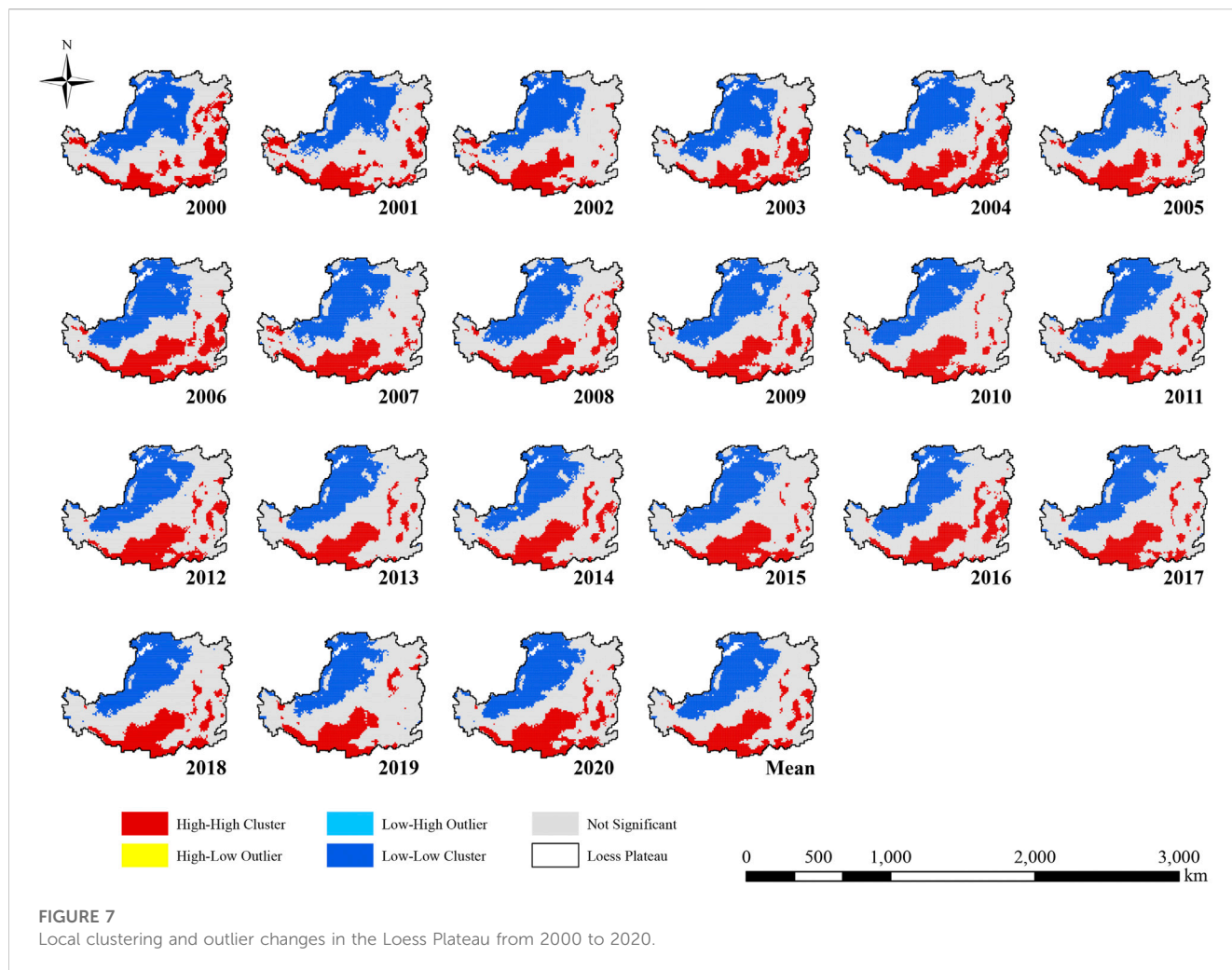
There was a positive correlation between NPP and precipitation in 94.09% of the LP, with only approximately 5.91% of the region revealing a negative correlation (Figure 8). A total of 58.92% of the regions had a significant positive correlation, mainly in Inner Mongolia, Ningxia and Shaanxi, southern Gansu and western Shanxi, and 35.17% of the regions showed significant irrelevance. Conversely, 5.90% of the regions showed no significant negative correlation, these areas were concentrated in Xi'an, southeastern Baoji in Shaanxi, and Sanmenxia and Luoyang in Henan, there were almost no significant negative correlations.

Compared with the variations in response to precipitation, the temperature influences on vegetation NPP in the LP were not obvious over many years. In terms of spatial distribution, 76.99% of the regions showed a positive correlation, while 23.01% showed a negative correlation. There were almost no

significant positive or negative correlations in the LP, as demonstrated in Figure 9.

In the study area, 73.73% of the regions showed an insignificant positive correlation, mainly in the southeast of Gansu Province, Ningxia, and Shanxi Province. Conversely, 22.86% of the region showed an insignificant negative correlation, in Yan'an, Xianyang, and Xi'an in the Shaanxi Province (Figure 9). The results indicate the impact of temperature rise on vegetation NPP has not had significant effects.

To further quantitatively explore the contributing factors to the vegetation NPP on the LP, we used correlation analyses. We compared the *p*-values of the correlation coefficients of precipitation and temperature; the least significant correlation coefficient was extracted as the highest value correlation coefficient (Figure 10). The two climatic factors (temperature and precipitation) on the LP and the highest significant NPP correlation revealed significant correlations in 48.96% of the regions, mainly in the northwest and northeastern Shanxi, with no significance in the southeast LP. A total of 48.96% of the NPP on LP was significantly influenced by temperature and precipitation, mainly in the northwest and northeast of Shanxi, while the influence of climatic factors was insignificant on NPP in the south and east



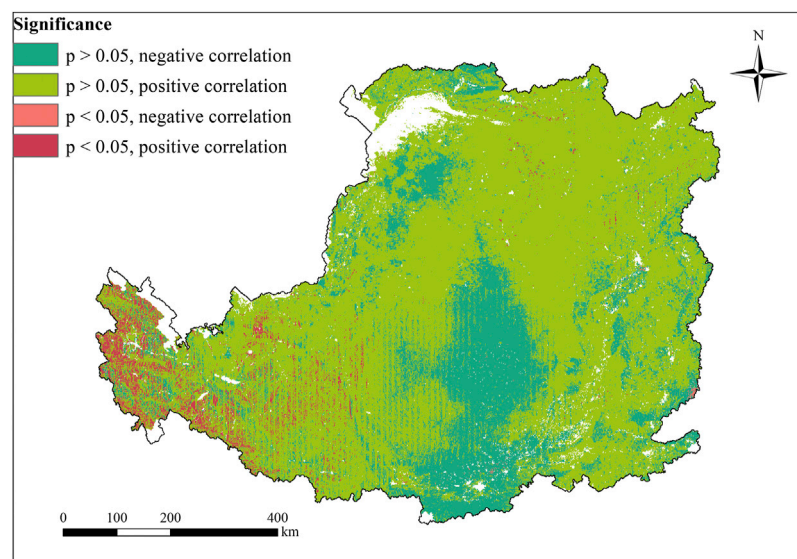


**FIGURE 9**  
Spatial distribution of the Pearson correlation results between net primary productivity and temperature in the Loess Plateau from 2000 to 2020.

of the LP (Figure 10A). On the LP, 86.31% of the area is heavily dependent on precipitation for vegetation NPP, whereas only 13.70% of the area relies mainly on temperature. Therefore, precipitation is the main climatic factor affecting variations in vegetation NPP on the LP (Figure 10B). Moreover, for provinces and cities, the areas mainly influenced by temperature were the Shaanxi Province (Xianyang, Tongchuan, Baoji, Xi'an), Guyuan City in Ningxia, Pingliang City in Gansu, Xining City in Qinghai, and Sanmenxia City in Henan, while other areas were mainly influenced by precipitation factors.

## 4 Discussion

### 4.1 Spatiotemporal variation in vegetation NPP

The interannual variation in NPP had “multi-peak” fluctuation increases since the implementation of the Grain for Green project on the LP. These peaks may be attributed to ecological engineering coupled with the effects of climate change and human activities. With global warming over the past 20 years, the climate of the LP has gradually increased in temperature and humidity; temperature and precipitation play an important role in vegetation growth (Sun et al., 2020). Additionally, many ecological construction projects have been implemented, including the natural forest protection project, the comprehensive management of small watersheds, and the Grain for Green Project. From artificial afforestation to natural restoration, the LP has an obvious “greening” trend (Li et al., 2017; Zhao et al., 2018; Deng and ShangGuan, 2021), thereby enhancing the carbon sequestration capacity of the vegetation. Our results are in line with previous findings (Feng et al., 2013; Jiang et al., 2019).

Interestingly, there are three distinct spikes in the NPP (2001–2002, 2011–2012, and 2017–2018). On the regional scale, the sudden increase in NPP from 2001 to 2002 corresponded with the pilot projects in Shaanxi and Gansu in 1999. After 2000, the pilot projects of returning farmland to forests were expanded to include 17 provinces in the central and western regions. The wave of forestry projects has continued, and vegetation growth improved as plants develop. The extreme NPP during 2011–2012 may be due to two factors, the implementation of a new round of Grain for Green Projects and sudden change in extreme temperatures which accelerated vegetation growth and abundance, improving NPP (Liu P. et al., 2022). In 2017, the State Council approved the conversion of Cropland to forests and grasslands in 17 provinces to expand the scale of agriculture and forestry in the region. The State Council also initiated rural revitalization and the mountains-rivers-forests-farmlands-lakes-grasslands program has favorably promoted the grand vision of “green waters and green mountains” (Li and Liu, 2022), which led to a sudden rise in NPP from 2017 to 2018. Moreover, the extreme precipitation levels correlated with NPP, especially the P-min with NPP, indicating that extreme precipitation may have strongly influenced the sudden increase in NPP (Figure 11). Similarly, at the provincial scale, the timing of sudden increases in vegetation NPP in each province also clustered with the three stages of distinct spikes. For example, the NPP in Shaanxi Province increased by  $72.21 \text{ gCm}^{-2} \text{ yr}^{-1}$  from 2001 to 2002, indicating that increased vegetation effectively controlled soil erosion, reduced carbon loss from the ecosystem, and enhanced carbon fixation.

The annual average vegetation NPP on the LP had a significant gradient from southeast to northwest. The area with an NPP above  $400 \text{ gCm}^{-2} \text{ yr}^{-1}$  gradually increased, and moved northward, with the main concentration in northern Shaanxi and southeastern Gansu and the Lüliang mountains in Shanxi. These results are in line with those of Zhang et al.

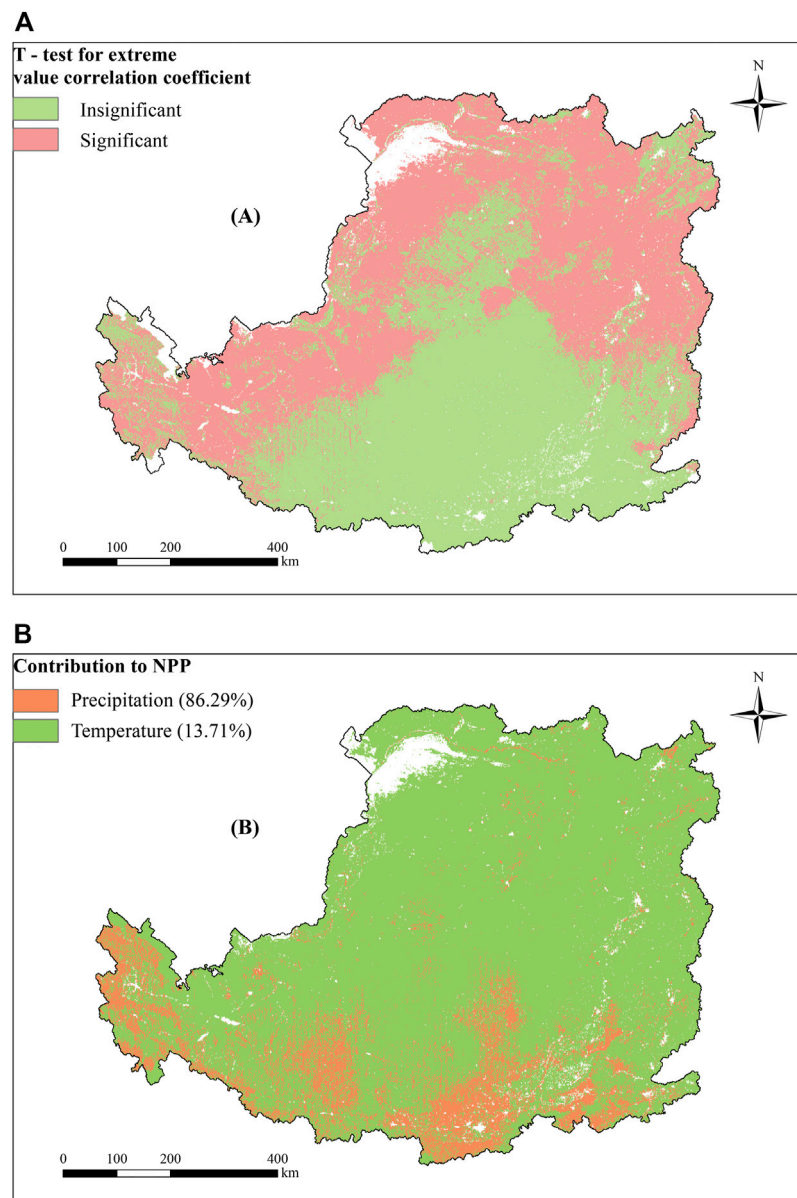


**FIGURE 10**

Spatial distribution **(A)** of the most significant correlation coefficients from the *t*-test results with precipitation and temperature; **(B)** contributions of precipitation and temperature to the significant net primary productivity results on the Loess Plateau for 2000–2020.

(2016). The higher NPP locations are the key restoration areas of the early pilot sites of the Grain for Green project. The pilot areas focused on the sub-region with warm temperate deciduous oak forest, with relatively superior site conditions as identified through superb afforestation technology, to ensure vegetation restoration success. However, the poor natural conditions, lack of water resources, severe drought, and planting a vegetation monoculture (single species) have allowed unused land to occupy most of the LP, impacting afforestation attempts in Inner Mongolia, Gansu, and Ningxia, resulting in slow NPP growth. In general, a series of large-scale ecological construction projects implemented over the past 21 years has changed the ecological environment of the LP and promoted the

sustainable development of the Yellow River Basin; the effect of the extensive vegetation restoration work was also outstanding.

#### 4.2 Effects of spatial autocorrelation on climate and human activities

Most previous studies have focused on the linear relationship and driving factors based on the “first-order effect,” ignoring the advantage of spatial autocorrelation which can remove the assumption of sample independence in classical statistics and performs well with potentially dependent samples. Presently, few studies have used the spatial

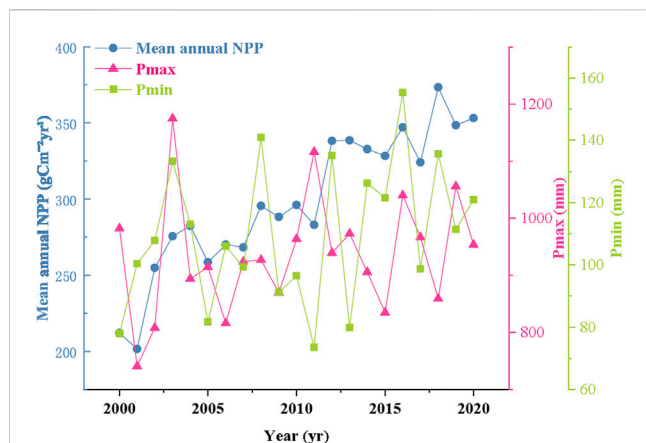


**FIGURE 11**  
Association between vegetation net primary productivity and extreme precipitation levels on the Loess Plateau from 2000 to 2020.

autocorrelation method to analyze spatial variation in NPP (Ren et al., 2020). Therefore, we used the “second-order effect” via spatial grid to explore the spatial correlation and heterogeneity of NPP in the LP. Our results reveal that the NPP of the LP from 2000 to 2020 had a strong spatial positive correlation ( $p < 0.01$ ), and an agglomeration effect, indicating that the ecosystems between the regions are not independent, yet interrelated with a tendency to gather. To avoid global autocorrelation masking local anomalies or instability, we explored the degree of local spatial aggregation on the LP and observed obvious polarization of cold and hot spots. The local spatial pattern of the LP is dominated by HH and LL clustering patterns, with a prominent hot spot area ( $p < 0.01$ ), which is similar to previous research (Wang and Gong, 2022). The HH is dominated by forests and cultivated land with vast carbon storage and is located in the warm temperate zone, which allows for an effective carbon sequestration. Focused conversion of farmland to forests involved sloping farmland converted into forest and grassland; the net forest area increased to 4,726 km<sup>2</sup> in 2020 (Table 4). Forests promote the accumulation of forest carbon and areas with high forest cover have significantly higher NPP than other habitats. In

the past 21 years, Ordos and Bayannur (cities in Inner Mongolia, northern Ningxia) and Baiyin City in the Gansu Province remain a LL district (cold spot), as previously indicated (Ren et al., 2020). The carbon sequestration services of ecosystems in the northwest of the LP remain low, with the fragile ecological environments impacting the success of vegetation restoration in this area.

The transfer matrix revealed the worst land categories (unused land and grassland) in Inner Mongolia, which accounted for 79.58% (Table 4) of this land category. In addition, the location is a temperate desert steppe zone with serious desertification of Mu Us sandy land. The ongoing coal mining in the Ordos City has also adversely impacted local vegetation and caused soil erosion.

Recently, the government has improved the area through ecological restoration, although vegetation rehabilitation remains slow (Wu et al., 2022).

To further explore the heterogeneity in the clustering patterns, we calculated the clustering patterns between counties and combined the annual average NPP of each county with LULC data to explore the abnormal changes between HH and LL and the significance levels of each stage.

The main reason for the disappearance of the LL in Ansai, Wuqi, Yanchang County, and Yan’an City in the Shaanxi Province and Shanxi (Xi and Yonghe County) from 2000 to 2005 was the transformation of sloping farmland into forest and grassland and of unused land into grassland, which increased the vegetation cover. The reason for the disappearance of the HH in Shanxi Province may be attributed to the conversion of grassland to cultivated land and the expansion of cultivated land to impervious surfaces, including the transfer of 76 km<sup>2</sup> in Yuanping County (from 2000 to 2005).

The main reason for the disappearance of HH from 2005 to 2010 was the transfer of cropland and grassland to impervious surfaces in some counties in Shanxi Province. For example, 11 km<sup>2</sup> of cropland and grassland in Gaoping County was changed to impervious surfaces. The expansion of urban construction has accelerated urbanization, thereby reducing the ability for vegetation to sequester carbon in many arable lands and grasslands. The emergence of LL is mainly the degradation of grassland. For example, the grassland was converted into unused land in Hangjin Banner in Inner Mongolia, creating an additional

**TABLE 4** Land use transfer matrix of the Loess Plateau from 2000 to 2020 (km<sup>2</sup>).

Land use type		2020						
		Cropland	Forest	Grassland	Unused land	Wetlands	Impervious surface	Water
2000	Cropland	181,132	1,383	7,279	1,796	654	4,712	464
	Forest	276	90,253	308	53	7	30	11
	Grassland	11,439	2,880	206,731	4,161	431	1,688	261
	Unused land	7,976	1,140	12,596	74,454	509	815	153
	Wetlands	58	3	4	33	1,228	4	18
	Impervious surface	0	0	0	0	0	8,706	0
	Water	37	5	11	4	58	4	1,414

90 km<sup>2</sup> of unused land from 2005 to 2010. The conversion of unused land to forest and grassland (in 2010–2015) was the main reason for the disappearance of the LL. Other clusters were less affected by land use changes. The disappearance of the LL in 2015–2020 and the expansion of the HH may be related to the transfer of grassland to cropland.

The local spatial anomaly of the NPP in the LP is driven by human-land relationship and natural factors. The effect of temperature on NPP was much smaller than that of precipitation, which is consistent with the results of Xie et al. (2014), however, Xie et al. (2014) did not provide the specific spatial distribution of NPP which is affected by climate indicators. This study revealed a positive correlation between NPP and precipitation in 94.09% on the LP, which indicates that precipitation has a strong synergy with plant photosynthesis and vegetation growth. The increased precipitation in the Qinling Mountains did not correspondingly increase the NPP or reduce vegetation resilience. Northwest China (especially Inner Mongolia, Gansu, and Shaanxi) is in arid and semi-arid areas. The lack of precipitation weakens the net primary production capacity of the vegetation, which might have caused consistent LL in the area. The quantitative results of the extreme value analysis revealed that the contribution of precipitation to NPP reached 86.31%; therefore, precipitation was the dominant climatic factor affecting variations in NPP in the LP. Combined with spatial autocorrelation analysis, the cold spot area was mainly influenced by precipitation, while the temperature had a stronger correlation with the hot spot area. This suggests that precipitation plays a decisive role in vegetation change in arid and semi-arid areas in the northwest of the LP, which is consistent with previous research on the impact of climate change on vegetation NPP in China (Ge et al., 2021). The southeast LP is in a warm temperate zone with abundant precipitation where vegetation growth is strongly affected by light conditions.

Our analysis of precipitation impacts identified a very close synergistic relationship between the interannual variation in NPP mean and minimum precipitation levels on the LP. There is both coordination and a tradeoff between the minimum and maximum precipitation.

The year of the tradeoff between the NPP and maximum precipitation almost coincides with the abnormal year in the local clustering model in the Shanxi and Henan provinces, which indicates that the heterogeneity of this spatial clustering model was affected by P-max (Figure 11). Hence, future studies should focus on the impact of extreme precipitation on vegetation restoration (Fischer et al., 2013).

The spatial autocorrelation model is based on the first law of geography and regularly applied in various industries. However, in ecology (especially in the application of remote sensing data) some mechanistic discussions have not been fully investigated. For example, Geoda and ArcGIS software is superior to previous ecological research which has not clearly defined data distance and the selection and rationality of thresholds, such as NPP.

This study focused on a single variable in the spatial autocorrelations to reveal the spatial variation in vegetation NPP on the LP. Future studies should combine multivariate spatial correlation analysis with economic, natural, and other indicators to explore the high and low clustering relationship between the factors and vegetation NPP to advise effective ecological construction.

Global warming remains a major global challenge. As an ecologically fragile area, we focused on temperature and rainfall as the natural factors influencing LP and identified gaps in the land cover data in a specific year. There may be deficiencies in our selection of indicators. Previous research has suggested that altitude and species diversity can also impact vegetation NPP. In the future, we will increase the diversity of valuable indicators in our exploration of the driving forces in vegetation carbon sequestration capacity to achieve the dual-carbon goal in China and the world.

In general, the vegetation NPP in the LP possessed a strong spatial autocorrelation. This spatial heterogeneity and dependence are driven by both natural factors and human activities. The results reveal that extreme NPP are a response to natural factors and violent disturbances by human activities and clarify the driving mechanism underlying vegetation carbon sequestration on the LP, revealing the spatial dependence of vegetation NPP and relationships between regions to support ecological management plans and provide suggestions to formulate double carbon plans. Future studies and relevant government departments should focus on fragile areas for vegetation restoration and, using the results of this study, accurately identify these vulnerable locations. By exploring the driving factors in vegetation restoration in each county, the correlations between the vegetation restoration impacts on the adjacent areas in space can be comprehensively explored. The potential future risks are predicted so that measures can be taken to prevent them. Reasonable regulation of land resources should solve issues of optimal allocation of space resources, which is especially important in the northwest region which has a weak vegetation carbon sequestration capacity, due to the inferior local conditions for ecological construction. Our results support the realization of ecological protection and high-quality development in the LP.

## 5 Conclusion

The average annual NPP of the LP showed an increasing trend with varying degrees. There was a sharp increase in the NPP over three periods. The spatial distribution pattern of NPP increased mainly in the middle and southeast of the LP. Furthermore, the average annual NPP of different types of vegetation increased significantly, while the unused land had great potential for carbon sequestration. The NPP of vegetation in the study area has a strong spatial correlation ( $p < 0.01$ ), and

the spatial clustering model is mainly HH and LL. HH accounts for 16%–22% of the LP, whereas LL accounts for 23%–30%.

Climate has a strong influence on vegetation NPP; however, recently the frequent land transformation due to human activities has greatly disturbed the spatial distribution of vegetation ecosystems. Additionally, changes among HH, LL, and insignificant areas are greatly affected by LUCC. The contribution of precipitation to regional NPP is much higher than temperature. Moreover, there is a strong synergistic relationship between the minimum value of precipitation and annual NPP. Future ecological management and decision makers should consider land planning and the important role of water resource allocation on vegetation growth. Finally, addressing problems such as the insufficient vegetation carrying capacity in the LP, and providing feasible schemes for green, low-carbon, and high-quality development of the LP remain to be accomplished.

## Data availability statement

The original contributions presented in the study are included in the article/[Supplementary Material](#), further inquiries can be directed to the corresponding author.

## Author contributions

SM: conceptualization, methodology, formal analysis, investigation, data curation, writing—original draft. ZS: conceptualization, methodology, validation, supervision, writing—review and editing, funding acquisition. All authors contributed to the article and approved the submitted version.

## References

- Anselin, L. (1995). Local indicators of spatial association—lisa. *Geogr. Anal.* 27, 93–115. doi:10.1111/j.1538-4632.1995.tb00338.x
- Chen, L. D., Huang, Z. L., Gong, J., Fu, B. J., and Huang, Y. L. (2007). The effect of land cover/vegetation on soil water dynamic in the hilly area of the loess plateau, China. *CATENA* 70, 200–208. doi:10.1016/j.catena.2006.08.007
- Cheniti, H., Cheniti, M., and Brahamia, K. (2021). Use of GIS and Moran's I to support residential solid waste recycling in the city of Annaba, Algeria. *Environ. Sci. Pollut. Res.* 28, 34027–34041. doi:10.1007/s11356-020-10911-z
- Cui, L. L., Shi, J., and Xiao, F. J. (2018). Impacts of climatic factors and El Niño/La Niña events on the changes of terrestrial ecosystem NPP in China. *Acta Geogr. Sin.* 73, 53–66. doi:10.11821/dlxb201801005
- Deng, L., and ShangGuan, Z. P. (2021). High quality developmental approach for soil and water conservation and ecological protection on the Loess Plateau. *Front. Agr. Sci. Eng.* 8, 501–511. doi:10.15302/j-fase-2021425
- Fan, C., and Myint, S. (2014). A comparison of spatial autocorrelation indices and landscape metrics in measuring urban landscape fragmentation. *Landsc. Urban Plann.* 121, 117–128. doi:10.1016/j.landurbplan.2013.10.002
- Feng, X. M., Fu, B. J., Lu, N., Zeng, Y., and Wu, B. F. (2013). How ecological restoration alters ecosystem services: An analysis of carbon sequestration in China's Loess Plateau. *Sci. Rep.* 3, 1–5. doi:10.1038/srep02846
- Fischer, E. M., Beyerle, U., and Knutti, R. (2013). Robust spatially aggregated projections of climate extremes. *Nat. Clim. Change* 3, 1033–1038. doi:10.1038/NCLIMATE2051
- Fu, B. J., Liu, Y., Lü, Y. H., He, C. S., Zeng, Y., and Wu, B. F. (2011). Assessing the soil erosion control service of ecosystems change in the Loess Plateau of China. *Ecol. Complex.* 8, 284–293. doi:10.1016/j.ecocom.2011.07.003
- Gbagir, A. M. G., Sikopo, C. S., Matengu, K. K., and Colpaert, A. (2022). Assessing the impact of wildlife on vegetation cover change, northeast Namibia, based on MODIS satellite imagery (2002–2021). *Sensors* 22.4006 doi:10.3390/s22114006
- Ge, W. Y., Deng, L. Q., Wang, F., and Han, J. Q. (2021). Quantifying the contributions of human activities and climate change to vegetation net primary productivity dynamics in China from 2001 to 2016. *Sci. Total Environ.* 773, 145648. doi:10.1016/j.scitotenv.2021.145648
- Getis, A., and Ord, J. K. (2010). *The analysis of spatial association by use of distance statistics, Perspectives on spatial data analysis*. Berlin, Germany Springer. pp 127–145.
- Goldewijk, K. K., and Leemans, R. (1995). *Systems models of terrestrial carbon cycling*. Berlin, Germany: Springer Berlin Heidelberg. pp 129–151.
- Guo, D., Song, X. N., Hu, R. H., Cai, S. H., Zhu, X. M., and Hao, Y. B. (2021). Grassland type-dependent spatiotemporal characteristics of productivity in Inner Mongolia and its response to climate factors. *Sci. Total Environ.* 775, 145644. doi:10.1016/j.scitotenv.2021.145644
- He, X. B., Zhou, J., Zhang, X. B., and Tang, K. L. (2006). Soil erosion response to climatic change and human activity during the Quaternary on the Loess Plateau. *China. Reg. Environ. Change.* 6, 62–70. doi:10.1007/s10113-005-0004-7
- Huang, Y., Wang, Y. J., Li, X. S., Hu, Z. L., and Liu, G. P. (2013). Graphic analysis of spatio-temporal effect for vegetation disturbance caused by coal mining: A case of datong coal mine area. *Acta Ecol. Sin.* 33, 7035–7043. doi:10.5846/stxb201207080952
- Jiang, H. C., and Ding, Z. L. (2005). Temporal and spatial changes of vegetation cover on the Chinese Loess Plateau through the last glacial cycle: Evidence from spore-pollen records. *Rev. Palaeobot. Palyno* 133, 23–37. doi:10.1016/j.revpalbo.2004.08.003
- Jiang, X. D., Shen, W., and Bai, X. Y. (2019). Response of net primary productivity to vegetation restoration in Chinese Loess Plateau during 1986–2015. *PLoS ONE* 14.e0219270 doi:10.1371/journal.pone.0219270

## Funding

This study was funded by the Major projects of the National Social Science Fund of China (22&ZD083).

## Acknowledgments

We would like to thank Editage ([www.editage.cn](http://www.editage.cn)) for English language editing.

## Conflict of interest

The authors declare that the research was conducted in the absence of any commercial or financial relationships that could be construed as a potential conflict of interest.

## Publisher's note

All claims expressed in this article are solely those of the authors and do not necessarily represent those of their affiliated organizations, or those of the publisher, the editors and the reviewers. Any product that may be evaluated in this article, or claim that may be made by its manufacturer, is not guaranteed or endorsed by the publisher.

## Supplementary material

The Supplementary Material for this article can be found online at: <https://www.frontiersin.org/articles/10.3389/fenvs.2023.1134917/full#supplementary-material>

- Kolby Smith, W., Reed, S. C., Cleveland, C. C., Ballantyne, A. P., Anderegg, W. R. L., Wieder, W. R., et al. (2016). Large divergence of satellite and Earth system model estimates of global terrestrial CO<sub>2</sub> fertilization. *Nat. Clim. Change* 6, 306–310. doi:10.1038/NCLIMATE2879
- Lei, T., Feng, J., Lv, J., Wang, J., Song, H., Song, W., et al. (2020). Net Primary Productivity Loss under different drought levels in different grassland ecosystems. *J. Environ. Manage.* 274, 111144. doi:10.1016/j.jenvman.2020.111144
- Li, C. H., Wang, Y. T., Wu, X. D., Cao, H. J., Li, W. P., and Wu, T. H. (2021). Reducing human activity promotes environmental restoration in arid and semi-arid regions: A case study in northwest China. *Sci. Total Environ.* 768, 144525. doi:10.1016/j.scitotenv.2020.144525
- Li, H. W., Ding, J. H., Zhang, J., Yang, Z. N., Yang, B., Zhu, Q., et al. (2020). Effects of land cover changes on net primary productivity in the terrestrial ecosystems of China from 2001 to 2012. *Land-Base* 9. doi:10.3390/land9120480
- Li, J. J., Peng, S. Z., and Li, Z. (2017). Detecting and attributing vegetation changes on China's Loess Plateau. *Agric. For. Meteorol.* 247, 260–270. doi:10.1016/j.agrformet.2017.08.005
- Li, S. D., and Liu, M. C. (2022). The development process, current situation and prospects of the conversion of farmland to forests and grasses project in China. *J. Resour. Ecol.* 13, 120–128. doi:10.5814/j.issn.1674-764x.2022.01.014
- Liu, H. X., Zhang, A. B., Jiang, T., Zhao, A. Z., Zhao, Y. L., and Wang, D. L. (2018). Response of vegetation productivity to climate change and human activities in the shaanxi-gansu-ningxia region, China. *J. Indian Soc. Remote* 46, 1081–1092. doi:10.1007/s12524-018-0769-z
- Liu, K., Liu, W. R., Wu, J. L., Chen, Z. F., Zhang, W., and Liu, F. (2022a). Spatial differences and influencing factors of urban water utilization efficiency in China. *Front. Environ. Sci.* 10, 593. doi:10.3389/fenvs.2022.890187
- Liu, P., Zhao, X. N., Gao, X. D., Yu, L. Y., and Ren, M. (2022b). Characteristics of extreme temperature variation in the Loess Plateau and its correlation with average temperature. *Chin. J. Appl. Ecol.* 33, 1975–1982. doi:10.13287/j.1001-9332.202207.024
- Liu, T. S., Guo, Z. T., Wu, N. Q., and Lu, H. Y. (1996). Prehistoric vegetation on the Loess Plateau: Steppe or forest? *J. S. Asian Earth* 13, 341–346. doi:10.1016/0743-9547(96)00041-4
- Lü, Y. H., Fu, B. J., Feng, X. M., Zeng, Y., Liu, Y., Chang, R. Y., et al. (2012). A policy-driven large scale ecological restoration: Quantifying ecosystem services changes in the Loess Plateau of China. *PLoS ONE* 7, e31782. doi:10.1371/journal.pone.0031782
- Ma, R. X., Wang, D. C., Cui, X. M., Yao, X. J., Li, S. S., Wang, H. S., et al. (2022). Distribution and driving force of water use efficiency under vegetation restoration on the Loess Plateau. *Remote Sens-Basel* 14. doi:10.3390/rs14184513
- Pan, J. H., and Dong, L. L. (2018). Spatio-temporal variation in vegetation net primary productivity and its relationship with climatic factors in the Shule River basin from 2001 to 2010. *Hum. Ecol. Risk Assess.* 24, 797–818. doi:10.1080/10807039.2017.1400373
- Pei, Y. Y., Huang, J. L., Wang, L. H., Chi, H., and Zhao, Y. J. (2018). An improved phenology-based CASA model for estimating net primary production of forest in central China based on Landsat images. *Int. J. Remote Sens.* 39, 7664–7692. doi:10.1080/01431161.2018.1478464
- Peng, J., Shen, H., Wu, W. H., Liu, Y. X., and Wang, Y. L. (2016). Net primary productivity (NPP) dynamics and associated urbanization driving forces in metropolitan areas: A case study in Beijing city, China. *Landsc. Ecol.* 31, 1077–1092. doi:10.1007/s10980-015-0319-9
- Ren, H. R., Shang, Y. J., and Zhang, S. (2020). Measuring the spatiotemporal variations of vegetation net primary productivity in Inner Mongolia using spatial autocorrelation. *Ecol. Indic.* 112, 106108. doi:10.1016/j.ecolind.2020.106108
- Shangguan, Z. P., and Zheng, S. X. (2006). Ecological properties of soil water and effects on forest vegetation in the Loess Plateau. *Int. J. Sustain. Dev. World Ecol.* 13, 307–314. doi:10.1080/13504500609469682
- Song, X. Z., Peng, C. H., Zhou, G. M., Jiang, H., and Wang, W. F. (2014). Chinese grain for green program led to highly increased soil organic carbon levels: A meta-analysis. *Sci. Rep.* 4, 1–7. doi:10.1038/srep04460
- Sun, R., Chen, S. H., and Su, H. B. (2020). Spatiotemporal variation of NDVI in different ecotypes on the Loess Plateau and its response to climate change. *Geogr. Res.* 39, 1200–1214. doi:10.11821/dlyj020190399
- Swetnam, T. L., Lynch, A. M., Falk, D. A., Yool, S. R., and Guertin, D. P. (2015). Discriminating disturbance from natural variation with LiDAR in semi-arid forests in the southwestern USA. *Ecosphere* 6, 1–22. doi:10.1890/Es14-00384.1
- Wang, T. F., and Gong, Z. W. (2022). Evaluation and analysis of water conservation function of ecosystem in Shaanxi Province in China based on “Grain for Green” Projects. *Environ. Sci. Pollut. Res.* 29, 1–19. doi:10.1007/s11356-022-21730-9
- Wang, Y. W., Yue, H. B., Peng, Q., He, C., Hong, S., and Bryan, B. A. (2020). Recent responses of grassland net primary productivity to climatic and anthropogenic factors in Kyrgyzstan. *Land Degrad. Dev.* 31, 2490–2506. doi:10.1002/ldr.3623
- Wei, X. D., Yang, J., Luo, P. P., Lin, L. G., Lin, K. L., and Guan, J. M. (2022). Assessment of the variation and influencing factors of vegetation NPP and carbon sink capacity under different natural conditions. *Ecol. Indic.* 138, 108834. doi:10.1016/j.ecolind.2022.108834
- Wu, D. H., Piao, S. L., Zhu, D., Wang, X. H., Ciais, P., Bastos, A., et al. (2020). Accelerated terrestrial ecosystem carbon turnover and its drivers. *Glob. Change Biol.* 26, 5052–5062. doi:10.1111/gcb.15224
- Wu, Q. Y., Yao, X. J., Liang, J., Zhang, S. L., Yang, Y. J., and Hou, H. P. (2022). Spatial and temporal intensity of vegetation cover improvement and degradation in coal mining areas of Erdos city. *J. Arid Land Resour. Environ.* 36, 101–109. doi:10.13448/j.cnki.jalre.2022.205
- Wu, S. H., Zhou, S. L., Chen, D. X., Wei, Z. Q., Dai, L., and Li, X. G. (2014). Determining the contributions of urbanisation and climate change to NPP variations over the last decade in the Yangtze River Delta, China. *Sci. Total Environ.* 472, 397–406. doi:10.1016/j.scitotenv.2013.10.128
- Xiao, F. J., Liu, Q. F., and Xu, Y. Q. (2022). Estimation of terrestrial net primary productivity in the Yellow River Basin of China using light use efficiency model. *Sustainability* 14, 7399. doi:10.3390/su14127399
- Xie, B. N., Qin, Z. F., Wang, Y., and Chang, Q. R. (2014). Spatial and temporal variation in terrestrial net primary productivity on Chinese Loess Plateau and its influential factors. *Trans. Chin. Soc. Agric. Eng.* 30, 244–253. doi:10.3969/j.issn.1002-6819.2014.11.030
- Yang, A. L., Zhang, X. P., Li, Z. S., Li, Y. C., and Nan, F. S. (2023). Quantitative analysis of the impacts of climate change and human activities on vegetation NPP in the Qilian Mountain National Park. *Acta Ecol. Sin.* 43, 1–9. doi:10.5846/stxb202202050295
- Yuan, S., Wang, Y. Q., Xu, J. J., and Wu, Z. G. (2021). Effects of climatic factors on the net primary productivity in the source region of Yangtze River, China. *Sci. Rep.* 11, 1–11. doi:10.1038/s41598-020-80494-9
- Zhang, B. Q., He, C. S., Burnham, M., and Zhang, L. H. (2016). Evaluating the coupling effects of climate aridity and vegetation restoration on soil erosion over the Loess Plateau in China. *Sci. Total Environ.* 539, 436–449. doi:10.1016/j.scitotenv.2015.08.132
- Zhang, M., Yuan, N. Q., Lin, H., Liu, Y., and Zhang, H. Q. (2022). Quantitative estimation of the factors impacting spatiotemporal variation in NPP in the Dongting Lake wetlands using Landsat time series data for the last two decades. *Ecol. Indic.* 135, 108544. doi:10.1016/j.ecolind.2022.109478
- Zhang, S. L., Yang, D. W., Yang, Y., Piao, S. L., Yang, H. B., Lei, H. M., et al. (2018). Excessive afforestation and soil drying on China's Loess Plateau. *J. Geophys. Res. Biogeosci.* 123, 923–935. doi:10.1002/2017JG004038
- Zhang, T., Peng, J., Liang, W., Yang, Y. T., and Liu, Y. X. (2016). Spatial-temporal patterns of water use efficiency and climate controls in China's Loess Plateau during 2000–2010. *Sci. Total Environ.* 565, 105–122. doi:10.1016/j.scitotenv.2016.04.126
- Zhang, X., Liu, L. Y., Chen, X. D., Gao, Y., Xie, S., and Mi, J. (2021). GLC\_FCS30: Global land-cover product with fine classification system at 30 m using time-series Landsat imagery. *Earth Syst. Sci. Data* 13, 2753–2776. doi:10.5194/essd-13-2753-2021
- Zhao, G. J., Mu, X. M., Wen, Z. M., Wang, F., and Gao, P. (2013). Soil erosion, conservation, and eco-environment changes in the Loess Plateau of China. *Land Degrad. Dev.* 24, 499–510. doi:10.1002/ldr.2246
- Zhao, H. F., He, H. M., Wang, J. J., Bai, C. Y., and Zhang, C. J. (2018). Vegetation restoration and its environmental effects on the Loess Plateau. *Sustainability* 10, 4676. doi:10.3390/su10124676
- Zhu, W. Q., Pan, Y. Z., and Zhang, J. S. (2007). Estimation of net primary productivity of Chinese terrestrial vegetation based on remote sensing. *Chin. J. Plant Ecol.* 31, 413. doi:10.3321/j.issn:1005-264X.2007.03.010